Terrestrial Water Loss at Night: Global Relevance from Observations and Climate Models

Ryan S. Padrón[1], Lukas Gudmundsson[1], Dominik Michel[1], Sonia I. Seneviratne[1]

[1]Institute for Atmospheric and Climate Science, Department of Environmental Systems Science, ETH Zurich, Zurich, 8092, Switzerland

Correspondence: Ryan S. Padrón (ryan.padron@env.ethz.ch)

Abstract. Nocturnal water loss (NWL) from the surface into the atmosphere is often overlooked because of the absence of solar radiation to drive evapotranspiration and the measuring difficulties involved. However, growing evidence suggests that NWL – and particularly nocturnal transpiration – represents a considerable fraction of the daily values. Here we provide a global overview of the characteristics of NWL based on latent heat flux estimates from the FLUXNET2015 dataset, as well as from simulations of global climate models. Eddy-covariance measurements at 99 sites indicate that on average NWL represents 6.3 % of total evapotranspiration. There are six sites where NWL is higher than 15 %; these are mountain forests with considerable NWL during winter related to snowy and windy conditions. Higher temperature, vapor pressure deficit, wind speed, soil moisture and downward longwave radiation are related to higher NWL, although this is not consistent across all sites. On the other hand, the global multi-model mean of terrestrial NWL is 7.9 % of total evapotranspiration. The spread of the model ensemble, however, is greater than 15.8 % over half of the land grid cells. Finally, NWL is projected to increase everywhere with an average of 1.8 %, although with a substantial inter-model spread. Changes in NWL contribute substantially to projected changes in total ET. Overall, this study highlights the relevance of water loss during the night and opens avenues to explore its influence on the water cycle and the climate system under present and future conditions.

1 Introduction

Water is lost from the surface to the atmosphere through evapotranspiration (ET). This process interlinks the water, energy and carbon cycles, and hence influences climate, ecology, agriculture, and economy (e.g. Betts et al., 1996; Fisher et al., 2017; Zhang et al., 2015). Although daytime ET, mainly driven by solar radiation, represents the majority of the contribution to total water loss, nighttime ET is likely non negligible. Nocturnal water loss may occur as evaporation from soil and canopy, snow sublimation, or plant transpiration through stomatal and cuticular conductance. It is also recognized that vapor pressure deficit, temperature, wind speed, longwave radiation and surface resistance influence nocturnal ET (Monteith, 1965; Penman, 1948). The prevalence of nocturnal water loss and its significance for the surface water and energy balance, however, remains overlooked and unclear.

In recent years there has been a growing body of evidence about the occurrence of nocturnal ET, with a specific focus on transpiration (Tr). Observations of nocturnal stomatal conductance across hundreds of species have challenged the assumption of stomatal closure in the absence of photosynthetically active radiation (e.g. Daley and Phillips, 2006; Dawson et al., 2007; Lombardozzi et al. 2017; Snyder et al., 2003). Possible advantages of nocturnal sap flow include capacitance

5   refilling, embolism removal, nutrient uptake, hydraulic redistribution and oxygen supply (Zeppel et al., 2014), whereas it remains unclear if Tr with no associated carbon gain has any benefits for vegetation or is simply unavoidable. Total water loss through ET, however, is more relevant than Tr from a water balance perspective since it additionally includes evaporation or snow sublimation from the ground and canopy. Nocturnal ET can be measured with lysimeters or eddy-covariance (EC) flux systems. A summary of previously reported nocturnal water loss estimates of both Tr and ET is

10   provided in Table 1.

Table 1. Nocturnal transpiration (Tr) and evapotranspiration estimates (ET) reported in the literature.

Nocturnal water loss	Measurement type	Vegetation type	Setup	Location	Reference
Tr (rate): 5–15 % of daytime rates typically, max: 30 %	Porometer, gas exchange, sap flow, lysimeter	Multiple C_3 and C_4 species	Field, lab, growth chamber, greenhouse	Multiple	Caird et al. (2007)
Tr: 10–25 % of total	Estimate from published literature	Typical plant functional types	Not available	Not available	Zeppel et al. (2014)
ET (annual): 3.5–9.5 % of daytime total	Lysimeter	Grass (plus shrub and moss)	Field	Western Germany	Groh et al. (2019)
ET: 12–23 % of daytime total	Lysimeter	Bean and cotton row-crops	Ecotron: controlled conditions	Montpellier (France)	de Dios et al. (2015)
ET: 6 % of total	Eddy-covariance	Oak - grass savanna	Field	California (US)	Fisher et al. (2007)
ET: 1 % of total	Eddy-covariance	Pinus Ponderosa forest	Field	California (US)	Fisher et al. (2007)
ET: 8–9 % of daytime total	Eddy-covariance	Grass field, Pine plantation, and hardwood forest	Field	Co-located sites in North Carolina (US)	Novick et al. (2009)

Water is not only lost from the surface during night, but it can also be gained by dew formation. For example, dew and hoar frost amounts to 4.2–6.4 % of annual precipitation in three humid grass sites in Austria and Germany (Groh et al., 2018,

15   2019), and was found to occur in approximately 30 % of the nights in a forest in central Colorado (Berkelhammer et al., 2013) and 70 % of the nights in a grassland in the Netherlands (Jacobs et al., 2006). ET and dew formation correspond to a latent heat flux and might both occur for example within an hour, proving difficult to disentangle them if the temporal resolution of the data is insufficient. In the present study, we therefore focus on the net latent heat flux or net nocturnal water loss (NWL) defined as ET minus dew formation.

Climate models generally represent latent heat flux as a function of the air-surface gradient in specific humidity and a resistance to water vapor transfer. This total resistance can include an aerodynamic resistance, a resistance to diffusion through the soil, a leaf boundary layer resistance and stomatal resistance. Stomatal resistance or conductance is

parameterized in most large-scale land surface models similarly to the Ball–Woodrow–Berry model (Ball et al., 1987; Ball, 1988; Collatz et al., 1991; Leuning, 1995; Medlyn et al., 2011; Sellers et al., 1996), i.e. as a linear function where the intercept is assumed to represent nocturnal conductance (see explanation in Lombardozzi et al., 2017). Meanwhile, new evidence suggests that nocturnal stomatal conductance is an actively controlled process, and that it is not equivalent to minimum conductance (Duursma et al., 2019). Underestimation of nocturnal stomatal conductance would lead to lower transpiration, and hence lower NWL. Previous research has noted that land surface models, dynamic global vegetation models and ecophysiological models continue to commonly assume that virtually no transpiration takes place at night, despite evidence suggesting otherwise (e.g. Lombardozzi et al., 2017; Zeppel et al., 2014). By adjusting the nocturnal stomatal conductance of the Community Land Model (CLM) version 4.5 based on empirical evidence, Lombardozzi et al. (2017) obtain an increase of up to 5 % in global transpiration, as well as significant effects on soil moisture availability and carbon uptake. In another study, Vinukollu et al. (2011) reported a mean nocturnal ET from the VIC land surface model of 9.6 % relative to daytime ET. It is also known that simple land evaporation models are not well suited for nocturnal conditions (Ershadi et al., 2014). Finally, to our knowledge, there have not been any studies analyzing NWL estimates from an ensemble of global climate models.

The goal of this study is to provide an overview of the magnitude and variability of NWL across the globe, as well as to explore its relationship to different meteorological and land cover conditions. An improved understanding of this overlooked flux is relevant for the surface water and energy balance. Until now most research about NWL stems from the plant physiology community, whereas the relevance of their results for hydrological and climate studies is yet to be fully explored. Here we analyze observations of NWL from a lysimeter and a global network of EC measurements, together with estimates from a climate model ensemble for present and projected future conditions. We conclude with a comparison of the observed and modeled data, while keeping in mind the stark difference in spatial resolution.

2 Data

2.1 Observations

2.1.1 Co-located lysimeter and EC station

Water fluxes are measured by a co-located weighing lysimeter and EC tower (2 m height) at the Rietholzbach pre-alpine catchment in Northeastern Switzerland (47.38° N, 8.99° E; 795 m a.s.l.; see Seneviratne et al., 2012 for site details). The sensors are thoroughly described by Hirschi et al. (2017). Given that in this case the focus is on sensor comparison, day and night are distinguished using a simple threshold of 10 W m^{-2} for measured incoming solar radiation below which it is assumed that no photosynthesis occurs (Hirschi et al., 2017). Data from 2010 to 2018 are used for comparing NWL estimates from these two independent measurement techniques.

For the lysimeter, changes in the total system mass (i.e. its weight plus accumulated seepage) are quantified every 5 minutes and correspond to water lost as ET or gained by precipitation, including dew. We apply an adaptive window and adaptive threshold (AWAT) filter to the total system mass of the lysimeter to reduce noise in the timeseries (Peters et al., 2014; Ruth et al., 2018). A minimum of 5 minutes and maximum of 45 minutes are assumed for the moving-average window, as well as a minimum of 0.01 mm and a maximum of 0.25 mm for the threshold values to distinguish signal from noise. A piecewise cubic Hermitian spline is used to interpolate between points of significant mass change (Peters et al., 2016), after applying an 85th percentile "snap routine" at inflection points (Peters et al., 2017). We estimate dew formation from hourly weight increases in the lysimeter when a co-located rain gauge does not record precipitation in that hour or the next. Note that very light precipitation might not be recorded due to the 0.1 mm rain gauge resolution. In those rare occasions when estimated dew surpasses a maximum formation rate of 0.07 mm h^{-1} (Monteith and Unsworth, 1990), it is instead attributed as rain or snow. NWL is calculated as ET minus dew. Lysimeter data from December to March are discarded because the quality is strongly affected by formation of snow bridges and the occurrence of snow drift. In addition, data from the following months are also omitted due to cases with unrealistic lysimeter weight and/or seepage measurements: July–September 2017, August 2014 and 2016, and November 2010, 2011 and 2016.

The EC data are processed with EddyPro (Fratini and Mauder, 2014; LI-COR, 2018) to obtain a latent heat flux time series with a temporal resolution of 30 minutes. Values are discarded for intervals when rain occurs, when the tower is in the upwind direction affecting the air flow (see Hirschi et al., 2017), and for cases with too low turbulence (median threshold for friction velocity) based on Wutzler et al. (2018). The resulting gaps are filled according to Reichstein et al. (2005). Latent heat flux is converted into water volume by dividing over the latent heat of vaporization; here we assume $\lambda = 2.472E6$ J kg^{-1}.

2.1.2 Global network of EC stations

To obtain a broader picture of NWL across the globe we employ the FLUXNET2015 Tier 1 dataset, which provides EC measurements of latent heat flux together with numerous other meteorological variables from a global network of 166 sites. We further select only those stations that contain at least 3 years of data to obtain a more accurate climatology of NWL. The temporal resolution of the data is 30 minutes. There are implemented tailored steps for quality assurance and quality control (Pastorello et al., 2014). A quality flag at each time interval indicates whether the data were measured or gap-filled based on marginal distribution sampling (Reichstein et al., 2005). Moreover, there is an energy balance closure correction factor applied to the data based on the assumption that the Bowen ratio is correct. A *joint uncertainty* estimate that combines a *random uncertainty* component and an energy balance closure component is provided at each timestep. Full details of the data processing are available at https://fluxnet.fluxdata.org/data/fluxnet2015-dataset/data-processing/. Even though the dataset distinguishes between daytime and nighttime intervals based on potential incoming solar radiation, we additionally determine the total number of nighttime hours by calculating the sunset and sunrise time of each day (see

https://www.esrl.noaa.gov/gmd/grad/solcalc/calcdetails.html). Finally, this study uses data from 99 sites (see Table A1) that include energy balance corrected measurements of latent heat flux, as well as the uncorrected fluxes.

Here we assume that the provided uncertainty for latent heat flux at each timestep i is the standard deviation (σ_i) of a normal distribution, and thus propagate it to obtain the uncertainty of the accumulated flux (σ_{sum}) over n timesteps as follows:

$$\sigma_{sum} = \left(\sum_{i=1}^{n} \sigma_i^2 + \sum_{j=1}^{n-1} \sum_{k=j+1}^{n} 2\rho_{jk}\sigma_j\sigma_k \right)^{0.5} \qquad (1),$$

where ρ_{jk} corresponds to the Pearson correlation between the estimates of timesteps j and k. Because there is no information available to compute this correlation, we assume an average $\rho_{jk} = 0$ in accordance with the FLUXNET2015 data processing. In addition, note that EC measurements do not account for latent heat storage in the air between the ground and measurement level. Lastly, it is important to be aware that the reliability of EC measurements decreases during the night due to low and intermittent turbulence (e.g. Baldocchi, 2003; Moffat et al., 2007). Nonetheless, on average across all analyzed sites, latent heat flux is measured in 60 % of all nighttime intervals, whereas gap-filling is required in the remaining 40 %.

2.2 Climate models

Sub-daily climate model output is required to study NWL. Here we analyze an ensemble of climate model simulations of the fifth phase of the Coupled Model Inter-comparison Project (CMIP5) that provide 3 hourly estimates of latent heat flux. As for the EC data, we obtain NWL by dividing it over the latent heat of vaporization λ. For present conditions we use data from historical simulations during the period 1976–2005, whereas for the future period 2081–2100, we use data from simulations with the "business as usual" RCP8.5 emissions scenario (Moss et al., 2010). The employed ensemble comprises 26 different models (or model configurations) with one initial condition simulation (see Table A2). Data from all models are bilinearly interpolated to a common 2.5° × 2.5° grid. Grid cells with data from less than 2/3 of all models are not considered.

To estimate total NWL we obtain the average flux from all 3 hourly intervals that are exclusively night, and then extrapolate this value based on the complete number of nocturnal hours. To achieve this, we compute the time of sunset and sunrise for each day at the center of each individual grid cell using the solar time equations without accounting for topography. Note that this extrapolation approach could lead to inaccuracies if the NWL rate from periods immediately following sunset or just prior to sunrise systematically differ from the NWL rate during the middle of the night.

3 Results

3.1 Observed nocturnal water loss

Monthly NWL from the co-located lysimeter and EC system show a Pearson correlation of 0.5 or 0.57, depending on how dew is estimated from the lysimeter data (L1 vs. L2, see Figs. 1a and 1b). For L1 (Fig. 1a), the default threshold of 0.07 mm

h^{-1} is used (Section 2.1.1). In the case of L2 (Fig. 1b), we select here as a sensitivity test a second threshold of 0.035 mm h^{-1}, i.e. half of the defined value of 0.07 mm h^{-1} for maximum dew formation, when processing the lysimeter data. Note that the correlations may be affected by the difference in the footprint of the sensors and periods with gap-filled EC data. Also, in this case there is no energy balance closure correction factor applied to the EC data. The agreement between EC and

5   lysimeter improves if the NWL monthly climatology is analyzed. Moreover, in months when one of the lysimeter estimates of NWL is either too high or too low relative to the EC data, the other lysimeter estimate generally has a much better agreement. Overall, these results suggest that EC measurements can provide meaningful estimates of NWL. The annual climatology of EC-based NWL at this particular grassland site in Switzerland is 34.3 mm, equivalent to 5.8 % of annual ET.
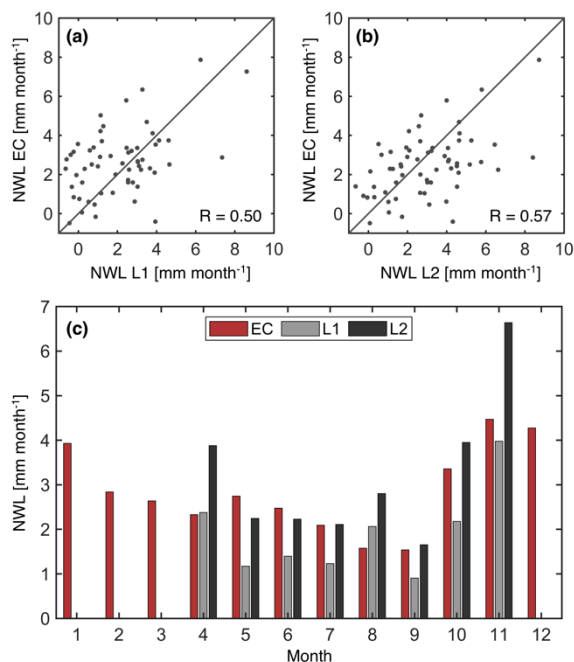
10   **Figure 1.** Comparison of nocturnal water loss (NWL) measured by the co-located lysimeter and EC system at Rietholzbach. Comparison of individual months is shown in (a) and (b) with the Pearson correlation coefficient denoted as R, whereas a comparison of the climatology from the period 2010–2018 is shown in (c). L1 corresponds to the lysimeter estimate with a maximum dew formation threshold of 0.07 mm h^{-1}, and L2 with a threshold of 0.035 mm h^{-1}. Lysimeter data from December to March are discarded because of measurements issues when snow is present.

15   An overview of observed NWL at the analyzed FLUXNET sites is presented in Fig. 2. Mean annual NWL based on energy balance corrected fluxes is 44.2 mm on average over all 99 stations, whereas the 5th and 95th percentiles of the distribution are 4.5 mm and 140.9 mm. There is a positive Spearman correlation coefficient of 0.61 between total ET and NWL, indicating generally higher NWL at sites with higher ET. The net nocturnal water loss as a fraction of total ET, i.e. NWL$_f$ = NWL / ET, provides more insight on the relevance of the nocturnal water flux. Average NWL$_f$ across all stations is 6.3 %,

20   the 5th percentile is 1 %, and the 95th percentile is 15.6 %. These annual mean values are computed from monthly climatologies obtained by omitting months with half or more of missing latent heat flux data. There is practically no difference in the distribution of NWL$_f$ with and without energy balance closure correction, whereas NWL is generally

smaller when based on uncorrected fluxes. Furthermore, the uncertainty of annual mean NWL_f per site, given by 2σ (~95 % confidence interval), is rather small with an average of ± 0.15 %. When assuming a more conservative value of $\rho_{jk} = 0.1$ in equation 1, the average uncertainty across sites increases to ± 1.7 %.

5   Interannual variability of NWL_f, represented by the standard deviation, is 2.4 % on average from all sites. To analyze seasonality, we compute NWL for the trimesters December–February (DJF), March–May (MAM), June–August (JJA) and September–November (SON) at all 81 sites located above 30° N, where seasonal differences are clearer, and data are available. The most common season with the highest NWL is winter (35.8 % of the sites) followed by autumn (25.9 %), summer (23.5 %) and spring (14.8 %); whereas for the lowest NWL, the most common is summer (37 %) and the least

10 common is autumn (13.6 %). Note that this is partly related to an increase in the total nocturnal hours as we go from summer to autumn and winter.
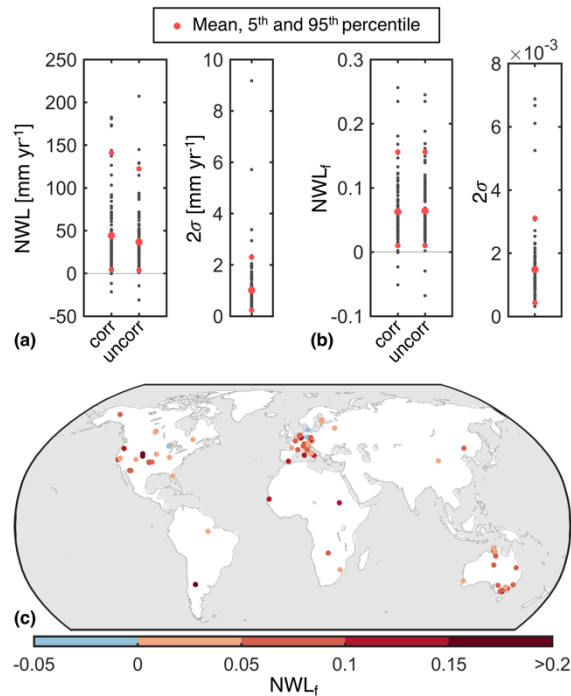
Figure 2. Nocturnal water loss at 99 FLUXNET sites as the annual NWL (a), and as the fraction of total evapotranspiration NWL_f (b). Values from individual sites are shown in black, whereas the mean, 5th percentile and 95th percentile are shown in red. Both energy balance
15 corrected values (corr) and uncorrected values (uncorr) are shown. Uncertainty estimates are given by 2σ, which correspond to a confidence interval of approximately 95 %. The uncertainty of total ET is small and therefore neglected when computing the uncertainty of NWL_f. (c) Location of sites with their estimated NWL_f.

The variability in NWL_f across sites cannot be easily explained by annual average climate conditions (temperature and precipitation) or land cover (Fig. 3). Nonetheless, deciduous broadleaf forests (DBF) have an overall lower NWL_f, whereas
20 evergreen needleleaf forests (ENF) include most cases with higher NWL_f. An ANOVA test (differences in the mean) for the

land cover categories has a p-value of 0.038, and a Kruskall-Wallis test (differences in the distribution) a p-value of 0.055. The three sites with negative NWL_f (dew is greater than nocturnal ET) are Hainich (Germany), Soroe (Denmark), and Willow Creek (WI, USA). These are all DBF with typically lower vapor pressure deficit and higher soil moisture than approximately 75 % of all sites. Moreover, it may be more difficult to accurately measure EC latent heat flux at DBF sites with large trees that reduce the ground-atmosphere coupling. On the other hand, there are six sites with $NWL_f > 15$ %: GLEES (WY, USA), GLEES Brooklyn tower (WY, USA), Niwot Ridge Forest (CO, USA), Lavarone (Italy), Wallaby Creek (Australia), and San Luis (Argentina). These are four ENF, an evergreen broadleaf forest (EBF) and a mixed forest (MF) in mountainous areas. Winter contribution to annual NWL approximately doubles that of summer in the four ENF sites. Snowier and windier conditions at these sites may suggest a considerable contribution of sublimation to NWL. The percentage of gap-filled data for these sites with relatively high or low NWL is not particularly different than for all other sites.
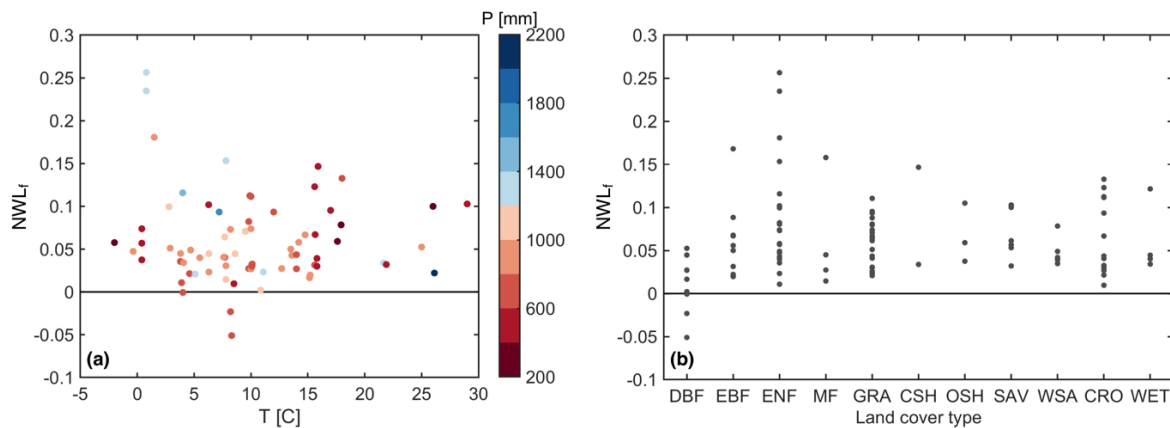
Figure 3. Relation of NWL_f with (a) mean annual temperature (T) and precipitation (P), and with (b) land cover type at FLUXNET sites. Precipitation and temperature data are available for 73 of the 99 FLUXNET sites. Land cover types are deciduous broadleaf forest (DBF), evergreen needleleaf forest (ENF), evergreen broadleaf forest (EBF), mixed forest (MF), grassland (GRA), closed shrubland (CSH), open shrubland (OSH), savanna (SAV), woody savanna (WSA), cropland (CRO), and wetland (WET).

At most sites there is a positive correlation of NWL with local air temperature (T), vapor pressure deficit (VPD), wind speed (WS), soil moisture (SM) and downward longwave radiation (LWd) for the 30-minute non-gap-filled data (Fig. 4). Correlations with net radiation (Rn) and ground heat flux (G) are also positive on average, but smaller. As expected, higher incoming energy (LWd, Rn, G), evaporative demand (T and VPD), aerodynamical conductance (related to WS) and water supply (related to SM) generally favor higher NWL. In addition, there is a tendency to have less NWL (i.e. latent heat flux) when sensible heat flux (SH) is higher, which is consistent with the partition of available energy. However, Spearman correlations at the majority of sites are smaller than 0.3. Reasons for this may include confounding effects among the analyzed drivers of NWL, observational uncertainty and a possible physiological control on nocturnal transpiration; e.g. the relationship of VPD with NWL might not increase monotonically if stomatal conductance decreases when VPD is high. Although there is no clear dependency of the correlations on land cover, we note that croplands (some of them irrigated)

often exhibit higher correlations with VPD and WS, while higher correlations with SM and LWd often correspond to short vegetation types. When analyzing data from summer months only, we find that correlations with VPD increase at forest sites, in particular at DBF. Also, the four sites with the highest correlations with SM are located in southern Arizona, an arid zone.
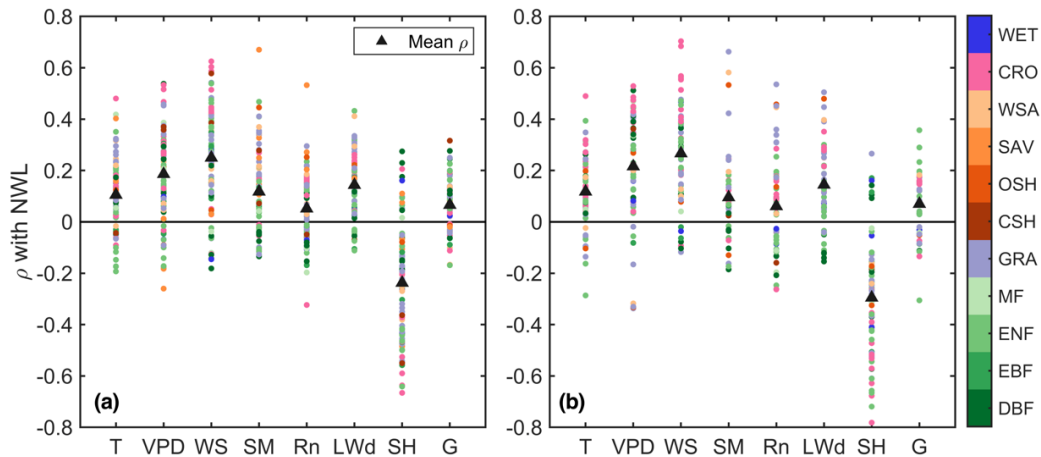
Figure 4. Spearman correlation (ρ) of 30-minute non-gap-filled nocturnal water loss (NWL) with air temperature (T), vapor pressure deficit (VPD), wind speed (WS), soil moisture (SM), net radiation (Rn), downward longwave radiation (LWd), sensible heat flux (SH) and ground heat flux (G) at FLUXNET sites. Panel (a) is for all data and (b) for summer months (JJA) at sites located above 30° N. Land cover types are deciduous broadleaf forest (DBF), evergreen needleleaf forest (ENF), evergreen broadleaf forest (EBF), mixed forest (MF), grassland (GRA), closed shrubland (CSH), open shrubland (OSH), savanna (SAV), woody savanna (WSA), cropland (CRO), and wetland (WET).

3.2 Climate model estimates of nocturnal water loss

The multi-model mean depicts an average NWL_f of 7.9 % across all land grid cells excluding desert regions and Greenland (Fig. 5). The 5th percentile of the spatial distribution without deserts and Greenland is 1.8 %, and the 95th percentile is 13.2 %. In tropical regions NWL_f is generally below the global average, even though NWL can e.g. surpass 80 mm yr^{-1} in parts of the Amazon. Central and northern Europe, USA, China and India show similar regional averages of approximately 9 %. The models also suggest a high relevance of nocturnal water fluxes in Australia with an average NWL_f of 13.1 %, and in the Mediterranean with 12 %. In most of Greenland and parts of Egypt the amount of dew or hoar frost is greater than the water lost through ET during the night. Interannual variability of NWL_f, given by the standard deviation of the 30-year time series from the multi-model mean, is below 2 % on 95 % of land grid cells excluding deserts and Greenland. Finally, we focus in the northern midlatitudes (30–60° N) to analyze seasonality. The multi-model mean indicates that autumn (SON) is the season with highest NWL on average (50.4 % of grid cells), whereas the lowest NWL typically corresponds to winter (DJF) (73 % of grid cells).
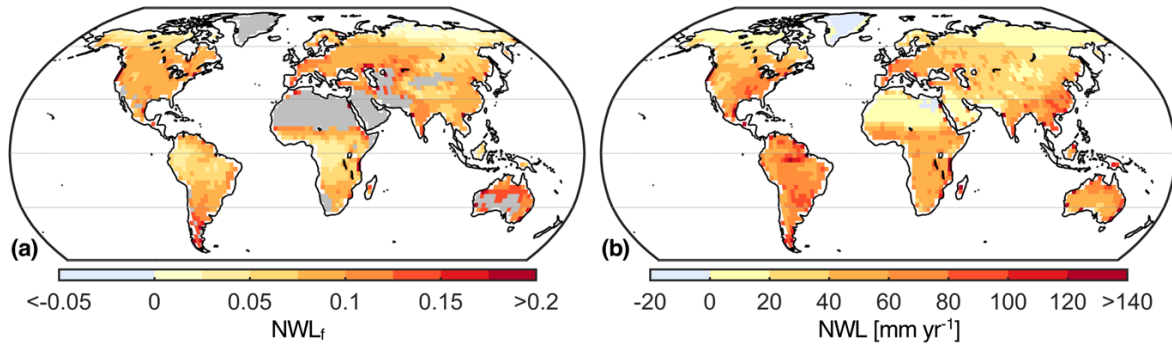
Figure 5. Map of multi-model mean NWL_f (a) and NWL (b) on average over the period 1976–2005. Desert regions and Greenland are masked in (a) because of division by small numbers.

There are large discrepancies in NWL_f between the different climate models (Fig. 6). The 95th percentile of the model

5 ensemble is higher than 15 % in most of the globe, whereas the 5th percentile even shows negative values (i.e. dew is greater than nocturnal ET) in parts of the tropics and high latitudes. The central 90 % spread of the ensemble is almost everywhere larger than 10 %, and even greater than 20 % in southern South America, eastern Africa, India and Australia. This means that at certain locations some models simulate NWL_f to be approximately zero, whereas estimates from other models are higher than 20 %. Even though the model differences in NWL_f can originate from differences in total ET (e.g. in India), we

10 also find differences in NWL generally ranging from 50 to 150 mm yr^{-1} (see Fig. S1).
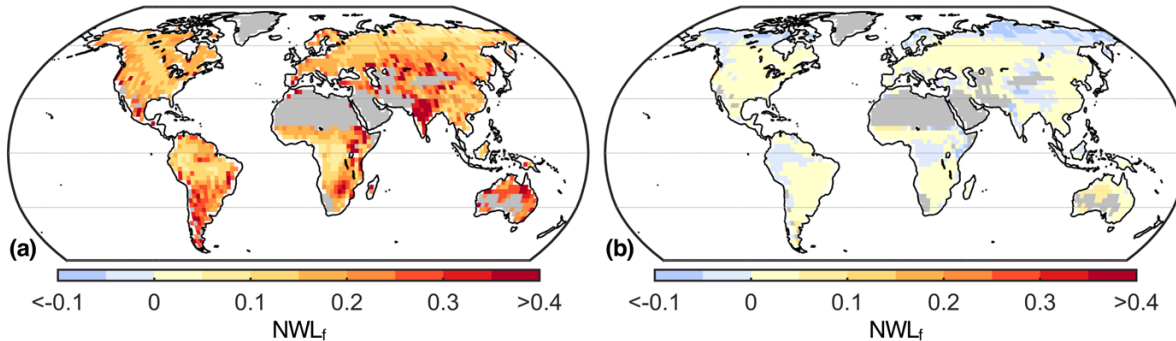
Figure 6. NWL_f uncertainty within the climate model ensemble. (a) Map of the 95th percentile of the ensemble. (b) Map of the 5th percentile of the ensemble. Desert regions and Greenland are masked because of division by small numbers.

The complexity of CMIP5 models, together with the fact that not all models are equally well documented, hinders a

15 straightforward assessment of potential factors contributing to the large inter-model differences in NWL. Nonetheless, we find a positive relation of climatological NWL and nighttime near-surface air temperatures across models (Fig. 7), indicating that models with high temperatures also tend to simulate high NWL. This correlation is present throughout the world and during the different seasons, although it decreases substantially in the Northern Hemisphere during summer (JJA). Furthermore, we note that inmcm4, EC-EARTH, NorESM1-M and CNRM-CM5 are models with systematically low values

of NWL throughout the globe; whereas GISS-E2-R, GISS-E2-H and MIROC5 tend to simulate the highest values of NWL (see Fig. S2).
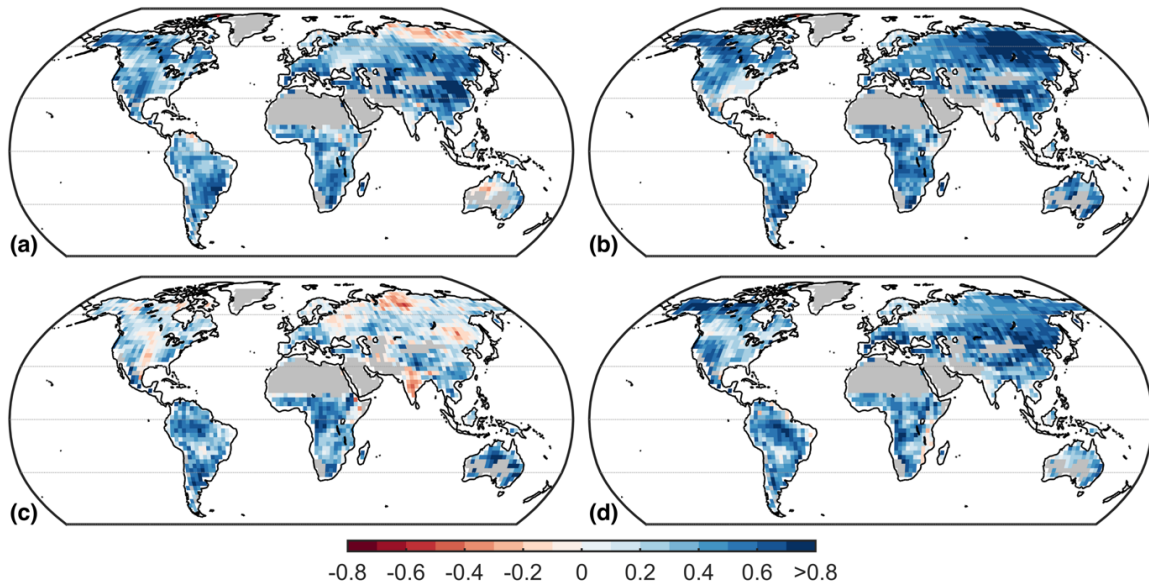
Figure 7. Pearson correlation at each grid cell between average NWL and nocturnal near-surface air temperature of climate models. Data corresponds to the period 1976–2005 from historical simulations. Correlations are computed separately for each season: (a) December–February, (b) March–May, (c) June–August, and (d) September–November. Desert regions and Greenland are masked for consistency.

Terrestrial NWL_f is projected to increase towards the end of the century throughout the globe (Fig. 8). The average increase in the multi-model mean is 1.8 %, neglecting deserts and Greenland. Whereas NWL is projected to increase almost everywhere, this is not the case for total ET. The increase in NWL_f in the Amazon, Central America, southern Africa and the Mediterranean is favored by a projected decrease in total ET. It is important to note that the spread of the model ensemble reduces confidence even in the sign of projected changes in NWL and total ET (Fig. S3). Lastly, we highlight the contribution of the nocturnal flux to projected changes in total ET. In more than half of all land grid cells, the projected change in NWL corresponds to 20 % or more of the absolute change in ET.
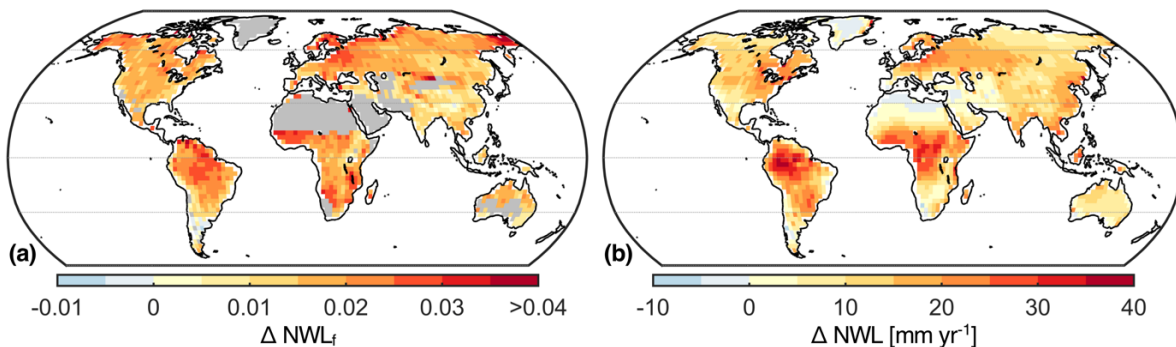
Figure 8. Multi-model mean of projected changes in NWL_f (a) and NWL (b) for the period 2081–2100 relative to the period 1976–2005. Desert regions and Greenland are masked in (a) because of division by small numbers.

3.3 Comparison of observed and simulated nocturnal water loss

We compare the site-level EC observations to model estimates from the corresponding grid cells, despite the large difference in spatial resolution. Modelled NWL_f generally shows an overestimation, although there are a few exceptions (Fig. 9a) – the average from the considered grid cells is 10.6 %, whereas the observational average is 7 %. Note once again the large discrepancies between individual models with an average spread of 20.5 % across locations calculated as the difference between the 97.5[th] percentile and 2.5[th] percentile. On the other hand, the estimated 95 % confidence interval of the EC observations is ± 0.15 % on average across sites. Interestingly, the multi-model mean has a smaller spread across sites than observations. This is partly explained by strong local discrepancies between individual models causing little variability in the multi-model mean; nonetheless, it could also be related to smoothing of cross-site differences in the much coarser spatial resolution of the models. At locations above 30° N, where most stations are found and seasonal differences are clearer, the simulated seasonal behavior agrees generally well with that of the EC data (Fig. 9b, see also Fig. S4). However, there is a noteworthy overestimation of the cases where the multi-model mean shows the lowest NWL to occur in summer, which is compensated by an underestimation for autumn and spring.
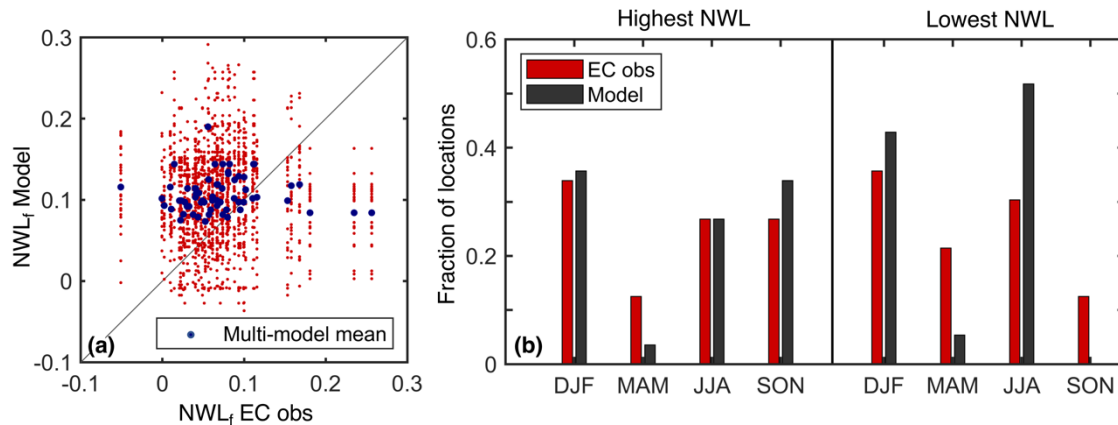
Figure 9. Comparison of observations with climate model simulations at the corresponding grid cells. (a) NWL_f from EC observations versus model simulations at 64 locations. (b) Fraction out of 56 locations (i.e. FLUXNET sites or grid cells) above 30° N where each season has the highest or lowest NWL on average. Seasons are defined by the trimesters December–February (DJF), March–May (MAM), June–August (JJA) and September–November (SON).

4 Discussion and conclusions

Our average estimate of net nocturnal water loss relative to total evapotranspiration from 99 FLUXNET sites is 6.3 %. This is smaller than reported values around 10–25 % from published physiological studies (Zeppel et al., 2014). However, it is important to distinguish that our focus is on the net flux, i.e. evapotranspiration minus dew, whereas physiological studies refer only to transpiration. The results agree with the expectation of lower NWL_f when dew is taken into account. In addition, we recall that nocturnal measurements at FLUXNET stations can be affected by low-turbulence conditions, and

therefore gap-filled and energy-balance-corrected data are used in the analysis. Future work could help to disentangle the distinct fluxes of transpiration, evaporation from soil and canopy, sublimation and dew during the night.

We find that higher air temperature, vapor pressure deficit, wind speed, soil moisture and downward longwave radiation tend to favor higher NWL, although the correlations are rather low. Similar results were reported by Groh et al. (2019) at two sites in Germany. Dawson et al. (2007) also found these conditions to favor higher nocturnal sap flow in woody plant species from different ecosystems, but in their case the relationships are much clearer. Meanwhile, Zeppel et al. (2014) point to plant functional type, ecosystem type, and biotic temporal characteristics like leaf or stand age, as possible additional factors influencing NWL. On the other hand, de Dios et al. (2015) found no temporal relation with vapor pressure deficit because of endogenous circadian regulation in an experiment with crops under controlled environmental conditions. Additionally, an increase in nocturnal sap flow and stomatal conductance was reported in two tree species under increased atmospheric CO_2 concentration, given sufficient soil moisture (Zeppel et al., 2011, 2012). Further research about the controls of NWL, and in particular nocturnal transpiration, is required.

The climate model ensemble provides an average NWL_f of 7.9 % over land, which is slightly higher than the observational estimate. Moreover, the overestimation is greater when considering only grid cells that contain FLUXNET sites. These relatively high multi-model mean estimates of NWL_f are surprising given the literature that suggests models underestimate nocturnal stomatal conductance (e.g. Lombardozzi et al. 2017; Zeppel et al., 2014). Note that increasing model nocturnal stomatal conductance would likely lead to even higher values of simulated NWL_f. Thus, it is possible that even if the mean simulated magnitude of nocturnal water loss is relatively accurate, the underlying processes may be misrepresented.

Our analysis indicates strong discrepancies between individual models in simulated NWL_f, which are much larger than the spatial and inter-annual variability. These discrepancies are related to differences in average nighttime temperature between models. Simulations that disentangle nocturnal transpiration, evaporation (sublimation) from soil and canopy, and dew would be highly relevant to study the inter-model differences. Note that differences in NWL can represent a substantial fraction of model differences in total ET. Furthermore, these biases could affect boundary layer evolution and precipitation timing in models. Inter-model uncertainty also reduces confidence in the direction of change in NWL under global warming, despite the multi-model mean showing a projected increase throughout the world.

In conclusion, our study provides a comprehensive global overview of NWL – defined as nocturnal evapotranspiration minus dew formation – from observations and climate models. The magnitude of this flux suggests it can be important for the surface energy and water balances, and therefore relevant to consider in hydroclimate analyses. Future research about NWL focused at seasonal and shorter timescales could address its influence on climate impacts during extreme conditions

(e.g., Duarte et al., 2016; Groh et al., 2019). Finally, ongoing development and expansion in sensing water and energy fluxes are expected to help address the uncertainties we have highlighted around NWL through continued research on this topic.

Data availability. The FLUXNET2015 Tier 1 dataset is available at https://fluxnet.fluxdata.org/data/fluxnet2015-dataset/.

5   Table A1 indicates the specific sites considered for the analysis. The CMIP5 data used in this study are available at https://esgf-node.llnl.gov/projects/esgf-llnl/. Detailed inputs for the search query are as follows: Model (see Table A2), Experiment (historical, rcp85), Time Frequency (3hr), Ensemble (see Table A2), Variable (hfls, tas). Processed hourly data from the co-located lysimeter and EC tower at Rietholzbach, as well as accompanying meteorological data, are available at https://doi.org/10.3929/ethz-b-000370968.

10   **Appendix A: List of FLUXNET sites and climate models used in the analysis**

Table A1. FLUXNET sites from the FLUXNET2015 dataset employed for the analysis. Included sites provide energy balance corrected measurements of latent heat flux during at least three years. The SITE_ID is indicated here, whereas a full description of each site is available at https://fluxnet.fluxdata.org/sites/site-list-and-pages/. Additionally, the number of years of data and average energy balance corrected NWL_f for each site is provided.

SITE_ID	# of years	NWL_f	SITE_ID	# of years	NWL_f	SITE_ID	# of years	NWL_f
AR-SLu	3	0.158	CN-HaM	3	0.026	IT-Tor	7	0.051
AT-Neu	11	0.023	CZ-wet	9	0.040	NL-Hor	8	0.074
AU-ASM	4	0.081	DE-Geb	14	0.010	NL-Loo	18	0.082
AU-Ade	3	0.042	DE-Gri	11	0.031	RU-Fyo	17	0.011
AU-Cpr	5	0.057	DE-Hai	13	-0.051	SD-Dem	5	0.100
AU-Cum	3	0.067	DE-Kli	11	0.041	SN-Dhr	4	0.103
AU-DaP	7	0.023	DE-Lkb	5	0.116	US-AR1	4	0.111
AU-DaS	7	0.053	DE-Obe	7	0.040	US-AR2	4	0.088
AU-Dry	7	0.061	DE-RuR	4	0.064	US-ARM	10	0.067
AU-Emr	3	0.081	DE-RuS	4	0.112	US-Blo	11	0.023
AU-Fog	3	0.122	DE-Seh	4	0.112	US-Cop	7	0.044
AU-Gin	4	0.041	DE-SfN	3	0.045	US-GBT	8	0.256
AU-How	14	0.035	DE-Tha	19	0.073	US-GLE	11	0.235
AU-RDF	3	0.049	DK-Sor	19	-0.023	US-KS2	4	0.034
AU-Rig	4	0.067	ES-LgS	3	0.105	US-Los	15	0.034
AU-Stp	7	0.061	FI-Hyy	19	0.036	US-MMS	16	0.002
AU-Tum	14	0.056	FI-Jok	4	0.021	US-Me2	13	0.102
AU-Wac	4	0.168	FR-Gri	10	0.093	US-NR1	17	0.181
AU-Whr	4	0.068	FR-LBr	13	0.043	US-Ne1	13	0.032

AU-Wom	3	0.088	FR-Pue	15	0.050	US-Ne2	13	0.030
AU-Ync	3	0.041	IT-BCi	11	0.133	US-Ne3	13	0.033
BE-Bra	19	0.027	IT-CA2	4	0.044	US-Prr	4	0.058
BE-Lon	11	0.027	IT-CA3	4	0.027	US-SRG	7	0.095
BE-Vie	19	0.015	IT-Col	19	0.045	US-SRM	11	0.078
BR-Sa3	5	0.022	IT-Cp2	3	0.020	US-Syv	14	0.045
CA-Qfo	8	0.047	IT-Cpz	13	0.031	US-Ton	14	0.039
CA-SF1	4	0.057	IT-Lav	12	0.153	US-Twt	6	0.123
CA-SF2	5	0.074	IT-MBo	11	0.021	US-Var	15	0.030
CA-SF3	6	0.038	IT-Noe	11	0.147	US-WCr	16	-0.001
CH-Cha	10	0.071	IT-PT1	3	0.027	US-Whs	8	0.059
CH-Dav	18	0.099	IT-Ren	16	0.049	US-Wkg	11	0.067
CH-Fru	10	0.093	IT-Ro2	11	0.017	ZA-Kru	11	0.032
CN-Cng	4	0.080	IT-SRo	14	0.058	ZM-Mon	10	0.053

Table A2. Climate models or model configurations employed for the analysis. Note that there are slightly variations depending on time period / scenario and on variable under consideration.

Model	Simulation	1976–2005: Historical		2081–2100: RCP8.5
		Latent heat flux	Temperature	Latent heat flux
ACCESS1-0	r1i1p1	X	X	X
ACCESS1-3	r1i1p1	X	X	X
bcc-csm1-1	r1i1p1	X	X	X
bcc-csm1-1-m	r1i1p1	X	X	X
BNU-ESM	r1i1p1	X	X	X
CCSM4	r6i1p1	X	X	X
CMCC-CM	r1i1p1	X	X	X
CNRM-CM5	r1i1p1	X	X	X
EC-EARTH	r2i1p1	X	X	X
FGOALS-g2	r1i1p1	X	X	X
FGOALS-s2	r1i1p1	X		
GFDL-CM3	r1i1p1	X	X	X
GFDL-ESM2G	r1i1p1	X	X	X
GFDL-ESM2M	r1i1p1	X	X	
GISS-E2-H	r6i1p1	X	X	X
GISS-E2-R	r6i1p1	X	X	X
HadGEM2-ES	r2i1p1	X	X	
inmcm4	r1i1p1	X	X	X

IPSL-CM5A-LR	r1i1p1	X	X	X
IPSL-CM5A-MR	r1i1p1	X	X	X
MIROC-ESM	r1i1p1	X	X	X
MIROC-ESM-CHEM	r1i1p1	X	X	X
MIROC5	r1i1p1	X	X	X
MRI-CGCM3	r1i1p1	X	X	X
MRI-ESM1	r1i1p1	X	X	
NorESM1-M	r1i1p1	X	X	X

Author contributions. RSP, LG and SIS conceived the idea and designed the study. SIS acquired the funding to carry out the research. DM collected and processed the co-located lysimeter and EC data from the Swiss site. RSP processed the FLUXNET2015 and CMIP5 data. RSP performed the analysis and wrote the manuscript with contributions from all authors throughout the study. All authors discussed the results, read and reviewed the manuscript.

Competing interests. The authors declare that they have no conflict of interest.

Acknowledgements

We acknowledge partial support from the H2020 CRESCENDO project (grant agreement 641816), and from the European Research Council (ERC) DROUGHT-HEAT project funded by the European Community's Seventh Framework Programme (grant agreement FP7-IDEAS-ERC-617518). This work used eddy covariance data acquired and shared by the FLUXNET community, including these networks: AmeriFlux, AfriFlux, AsiaFlux, CarboAfrica, CarboEuropeIP, CarboItaly, CarboMont, ChinaFlux, Fluxnet-Canada, GreenGrass, ICOS, KoFlux, LBA, NECC, OzFlux-TERN, TCOS-Siberia, and USCCC. The ERA-Interim reanalysis data are provided by ECMWF and processed by LSCE. The FLUXNET eddy covariance data processing and harmonization was carried out by the European Fluxes Database Cluster, AmeriFlux Management Project, and Fluxdata project of FLUXNET, with the support of CDIAC and ICOS Ecosystem Thematic Center, and the OzFlux, ChinaFlux and AsiaFlux offices. We appreciate the substantial and exhaustive work carried out to provide best estimates of the fluxes in the FLUXNET2015 dataset. We acknowledge the World Climate Research Program's Working Group on Coupled Modelling, which is responsible for the Coupled Model Intercomparison Project (CMIP), and we thank the climate modelling groups for producing and making available their model output. For CMIP, the US Department of Energy's Program for Climate Model Diagnosis and Intercomparison provides coordinating support and led development of software infrastructure in partnership with the Global Organization for Earth System Science Portals. The CMIP5 data used in this study are available at https://esgf-node.llnl.gov/projects/esgf-llnl/. We thank Urs Beyerle for downloading the CMIP5 data.

References

Baldocchi, D. D.: Assessing the eddy covariance technique for evaluating carbon dioxide exchange rates of ecosystems: past, present and future, Glob. Chang. Biol., 9(4), 479–492, doi:10.1046/j.1365-2486.2003.00629.x, 2003.

Ball, J. T.: An Analysis of Stomatal Conductance, Stanford University, 1988.

5 Ball, J. T., Woodrow, I. E., and Berry, J. A.: A Model Predicting Stomatal Conductance and its Contribution to the Control of Photosynthesis under Different Environmental Conditions, in: Progress in Photosynthesis Research, edited by: Biggins, J., 221– 224, Springer Netherlands, doi:10.1007/978-94-017-0519-6_48, 1987.

Berkelhammer, M., Hu, J., Bailey, A., Noone, D. C., Still, C. J., Barnard, H., Gochis, D., Hsiao, G. S., Rahn, T. and Turnipseed, A.: The nocturnal water cycle in an open-canopy forest, J. Geophys. Res. Atmos., 118(17), 10,225-10,242,

10   doi:10.1002/jgrd.50701, 2013.

Betts, A. K., Ball, J. H., Beljaars, A. C. M., Miller, M. J. and Viterbo, P. A.: The land surface-atmosphere interaction: A review based on observational and global modeling perspectives, J. Geophys. Res. Atmos., 101(D3), 7209–7225, doi:10.1029/95JD02135, 1996.

Caird, M. A., Richards, J. H. and Donovan, L. A.: Nighttime stomatal conductance and transpiration in C3 and C4 plants.,

15   Plant Physiol., 143(1), 4–10, doi:10.1104/pp.106.092940, 2007.

Collatz, G. J., Ball, J. T., Grivet, C., and Berry, J. A.: Physiological and environmental regulation of stomatal conductance, photosynthesis and transpiration: a model that includes a laminar boundary layer, Agr. Forest Meteorol., 54, 107–136, doi:10.1016/0168-1923(91)90002-8, 1991.

Daley, M. J. and Phillips, N. G.: Interspecific variation in nighttime transpiration and stomatal conductance in a mixed New

20   England deciduous forest, Tree Physiol., 26(4), 411–419, doi:10.1093/treephys/26.4.411, 2006.

Dawson, T. E., Burgess, S. S. O., Tu, K. P., Oliveira, R. S., Santiago, L. S., Fisher, J. B., Simonin, K. A. and Ambrose, A. R.: Nighttime transpiration in woody plants from contrasting ecosystems, Tree Physiol., 27(4), 561–575, doi:10.1093/treephys/27.4.561, 2007.

de Dios, V. R., Roy, J., Ferrio, J. P., Alday, J. G., Landais, D., Milcu, A. and Gessler, A.: Processes driving nocturnal

25   transpiration and implications for estimating land evapotranspiration., Sci. Rep., 5, 10975, doi:10.1038/srep10975, 2015.

Duarte, A. G., Katata, G., Hoshika, Y., Hossain, M., Kreuzwieser, J., Arneth, A. and Ruehr, N. K.: Immediate and potential long-term effects of consecutive heat waves on the photosynthetic performance and water balance in Douglas-fir, J. Plant Physiol., 205, 57–66, doi:10.1016/J.JPLPH.2016.08.012, 2016.

30 Duursma, R. A., Blackman, C. J., Lopéz, R., Martin-StPaul, N. K., Cochard, H. and Medlyn, B. E.: On the minimum leaf conductance: its role in models of plant water use, and ecological and environmental controls, New Phytol., 221(2), 693–705, doi:10.1111/nph.15395, 2019.

Ershadi, A., McCabe, M. F., Evans, J. P., Chaney, N. W. and Wood, E. F.: Multi-site evaluation of terrestrial evaporation

models using FLUXNET data, Agric. For. Meteorol., 187, 46–61, doi:10.1016/J.AGRFORMET.2013.11.008, 2014.

Fisher, J. B., Baldocchi, D. D., Misson, L., Dawson, T. E. and Goldstein, A. H.: What the towers don't see at night: nocturnal sap flow in trees and shrubs at two AmeriFlux sites in California., Tree Physiol., 27(4), 597–610 [online] Available from: http://www.ncbi.nlm.nih.gov/pubmed/17242001 (Accessed 20 November 2018), 2007.

5 Fisher, J. B., Melton, F., Middleton, E., Hain, C., Anderson, M., Allen, R., McCabe, M. F., Hook, S., Baldocchi, D., Townsend, P. A., Kilic, A., Tu, K., Miralles, D. D., Perret, J., Lagouarde, J.-P., Waliser, D., Purdy, A. J., French, A., Schimel, D., Famiglietti, J. S., Stephens, G. and Wood, E. F.: The future of evapotranspiration: Global requirements for ecosystem functioning, carbon and climate feedbacks, agricultural management, and water resources, Water Resour. Res., 53(4), 2618–2626, doi:10.1002/2016WR020175, 2017.

10 Fratini, G. and Mauder, M.: Towards a consistent eddy-covariance processing: an intercomparison of EddyPro and TK3, Atmos. Meas. Tech., 7(7), 2273–2281, doi:10.5194/amt-7-2273-2014, 2014.

Groh, J., Slawitsch, V., Herndl, M., Graf, A., Vereecken, H. and Pütz, T.: Determining dew and hoar frost formation for a low mountain range and alpine grassland site by weighable lysimeter, J. Hydrol., 563, 372–381, doi:10.1016/J.JHYDROL.2018.06.009, 2018.

15 Groh, J., Pütz, T., Gerke, H. H., Vanderborght, J. and Vereecken, H.: Quantification and Prediction of Nighttime Evapotranspiration for Two Distinct Grassland Ecosystems, Water Resour. Res., 55, 2018WR024072, doi:10.1029/2018WR024072, 2019.

Hirschi, M., Michel, D., Lehner, I. and Seneviratne, S. I.: A site-level comparison of lysimeter and eddy covariance flux measurements of evapotranspiration, Hydrol. Earth Syst. Sci, 21, 1809–1825, doi:10.5194/hess-21-1809-2017, 2017.

20 Jacobs, A. F. G., Heusinkveld, B. G., Kruit, R. J. W. and Berkowicz, S. M.: Contribution of dew to the water budget of a grassland area in the Netherlands, Water Resour. Res., 42(3), doi:10.1029/2005WR004055, 2006.

Leuning, R.: A critical appraisal of a combined stomatal-photosynthesis model for C3 plants, Plant, Cell Environ., 18(4), 339–355, doi:10.1111/j.1365-3040.1995.tb00370.x, 1995.

LI-COR Biosciences: Eddy Covariance Processing Software (Version 6.2.2) [Software]. Available at
25   www.licor.com/EddyPro, 2018.

Lombardozzi, D. L., Zeppel, M. J. B., Fisher, R. A. and Tawfik, A.: Representing nighttime and minimum conductance in CLM4.5: global hydrology and carbon sensitivity analysis using observational constraints, Geosci. Model Dev., 10, 321–331, doi:10.5194/gmd-10-321-2017, 2017.

Medlyn, B. E., Duursma, R. A., Eamus, D., Ellsworth, D. S., Prentice, I. C., Barton, C. V. M., Crous, K. Y., De Angelis, P.,
30   Freeman, M. and Wingate, L.: Reconciling the optimal and empirical approaches to modelling stomatal conductance, Glob. Chang. Biol., 17(6), 2134–2144, doi:10.1111/j.1365-2486.2010.02375.x, 2011.

Moffat, A. M., Papale, D., Reichstein, M., Hollinger, D. Y., Richardson, A. D., Barr, A. G., Beckstein, C., Braswell, B. H., Churkina, G., Desai, A. R., Falge, E., Gove, J. H., Heimann, M., Hui, D., Jarvis, A. J., Kattge, J., Noormets, A. and Stauch, V. J.: Comprehensive comparison of gap-filling techniques for eddy covariance net carbon fluxes, Agric. For.

Meteorol., 147(3–4), 209–232, doi:10.1016/J.AGRFORMET.2007.08.011, 2007.

Monteith, J. L.: Evaporation and environment, Symp. Soc. Exp. Biol., 19, 205–234, 1965.

Monteith, J. L. and Unsworth, M. H.: Principles of environmental physics. Arnold, London, UK, xii, pp. 291, 1990.

Moss, R. H., Edmonds, J. A., Hibbard, K. A., Manning, M. R., Rose, S. K., van Vuuren, D. P., Carter, T. R., Emori, S.,
Kainuma, M., Kram, T., Meehl, G. A., Mitchell, J. F. B., Nakicenovic, N., Riahi, K., Smith, S. J., Stouffer, R. J.,
Thomson, A. M., Weyant, J. P. and Wilbanks, T. J.: The next generation of scenarios for climate change research and
assessment, Nature, 463(7282), 747–756, doi:10.1038/nature08823, 2010.

Novick, K. A., Oren, R., Stoy, P. C., Siqueira, M. B. S. and Katul, G. G.: Nocturnal evapotranspiration in eddy-covariance
records from three co-located ecosystems in the Southeastern U.S.: Implications for annual fluxes, Agric. For.
Meteorol., 149(9), 1491–1504, doi:10.1016/j.agrformet.2009.04.005, 2009.

Pastorello, G. Z., Agarwal, D. A., Papale, D., Samak, T., Trotta, C., Ribeca, A., Poindexter, C. M., Faybishenko, B., Gunter,
D. K., Hollowgrass, R., Canfora, E.: Observational Data Patterns for Time Series Data Quality Assessment, Proc. 10th
IEEE International Conference on e-Science (e-Science'2014), Sao Paulo, pp. 271-278, doi: 10.1109/eScience.2014.45,
2014.

Penman, H. L.: Natural evaporation from open water, bare soil and grass, Proc. R. Soc. Lond. A. Math. Phys. Sci., 193
(1032), 120–145, 1948.

Peters, A., Nehls, T., Schonsky, H. and Wessolek, G.: Separating precipitation and evapotranspiration from noise-a new
filter routine for high-resolution lysimeter data, Hydrol. Earth Syst. Sci, 18, 1189–1198, doi:10.5194/hess-18-1189-
2014, 2014.

Peters, A., Nehls, T. and Wessolek, G.: Technical note: Improving the AWAT filter with interpolation schemes for advanced
processing of high resolution data, Hydrol. Earth Syst. Sci, 20, 2309–2315, doi:10.5194/hess-20-2309-2016, 2016.

Peters, A., Groh, J., Schrader, F., Durner, W., Vereecken, H. and Pütz, T.: Towards an unbiased filter routine to determine
precipitation and evapotranspiration from high precision lysimeter measurements, J. Hydrol., 549, 731–740,
doi:10.1016/J.JHYDROL.2017.04.015, 2017.

Reichstein, M., Falge, E., Baldocchi, D., Papale, D., Aubinet, M., Berbigier, P., Bernhofer, C., Buchmann, N., Gilmanov, T.,
Granier, A., Grunwald, T., Havrankova, K., Ilvesniemi, H., Janous, D., Knohl, A., Laurila, T., Lohila, A., Loustau, D.,
Matteucci, G., Meyers, T., Miglietta, F., Ourcival, J.-M., Pumpanen, J., Rambal, S., Rotenberg, E., Sanz, M., Tenhunen,
J., Seufert, G., Vaccari, F., Vesala, T., Yakir, D. and Valentini, R.: On the separation of net ecosystem exchange into
assimilation and ecosystem respiration: review and improved algorithm, Glob. Chang. Biol., 11(9), 1424–1439,
doi:10.1111/j.1365-2486.2005.001002.x, 2005.

Ruth, C. E., Michel, D., Hirschi, M. and Seneviratne, S. I.: Comparative Study of a Long-Established Large Weighing
Lysimeter and a State-of-the-Art Mini-lysimeter, Vadose Zo. J., 17(1), 0, doi:10.2136/vzj2017.01.0026, 2018.

Sellers, P. J., Randall, D. A., Collatz, G. J., Berry, J. A., Field, C. B., Dazlich, D. A., Zhang, C., Collelo, G. D., Bounoua, L.,
Sellers, P. J., Randall, D. A., Collatz, G. J., Berry, J. A., Field, C. B., Dazlich, D. A., Zhang, C., Collelo, G. D. and

Bounoua, L.: A Revised Land Surface Parameterization (SiB2) for Atmospheric GCMS. Part I: Model Formulation, J. Clim., 9(4), 676–705, doi:10.1175/1520-0442(1996)009<0676:ARLSPF>2.0.CO;2, 1996.

Seneviratne, S. I., Lehner, I., Gurtz, J., Teuling, A. J., Lang, H., Moser, U., Grebner, D., Menzel, L., Schroff, K., Vitvar, T. and Zappa, M.: Swiss prealpine Rietholzbach research catchment and lysimeter: 32 year time series and 2003 drought event, Water Resour. Res., 48(6), W06526, doi:10.1029/2011WR011749, 2012.

Snyder, K. A., Richards, J. H. and Donovan, L. A.: Night-time conductance in C3 and C4 species: do plants lose water at night?, J. Exp. Bot., 54(383), 861–865, doi:10.1093/jxb/erg082, 2003.

Vinukollu, R. K., Wood, E. F., Ferguson, C. R. and Fisher, J. B.: Global estimates of evapotranspiration for climate studies using multi-sensor remote sensing data: Evaluation of three process-based approaches, Remote Sens. Environ., 115(3), 801–823, doi:10.1016/J.RSE.2010.11.006, 2011.

Wutzler, T., Lucas-Moffat, A., Migliavacca, M., Knauer, J., Sickel, K., Šigut, L., Menzer, O. and Reichstein, M.: Basic and extensible post-processing of eddy covariance flux data with REddyProc, Biogeosciences, 15(16), 5015–5030, doi:10.5194/bg-15-5015-2018, 2018.

Zeppel, M. J. B., Lewis, J. D., Medlyn, B., Barton, C. V. M., Duursma, R. A., Eamus, D., Adams, M. A., Phillips, N., Ellsworth, D. S., Forster, M. A. and Tissue, D. T.: Interactive effects of elevated CO2 and drought on nocturnal water fluxes in Eucalyptus saligna, Tree Physiol., 31, 932–944, doi:10.1093/treephys/tpr024, 2011.

Zeppel, M. J. B., Lewis, J. D., Chaszar, B., Smith, R. A., Medlyn, B. E., Huxman, T. E. and Tissue, D. T.: Nocturnal stomatal conductance responses to rising [CO2], temperature and drought, New Phytol., 193(4), 929–938, doi:10.1111/j.1469-8137.2011.03993.x, 2012.

Zeppel, M. J. B., Lewis, J. D., Phillips, N. G. and Tissue, D. T.: Consequences of nocturnal water loss: a synthesis of regulating factors and implications for capacitance, embolism and use in models, Tree Physiol., 34(10), 1047–1055, doi:10.1093/treephys/tpu089, 2014.

Zhang, K., Kimball, J. S., Nemani, R. R., Running, S. W., Hong, Y., Gourley, J. J. and Yu, Z.: Vegetation Greening and Climate Change Promote Multidecadal Rises of Global Land Evapotranspiration, Sci. Rep., 5(1), 15956, doi:10.1038/srep15956, 2015.